

3D OBJECT RECONSTRUCTION USING A HIGH RESOLUTION HYBRID MEASUREMENT SYSTEM

Dieter Kraus, Claus Brenner, Dieter Fritsch
Institute for Photogrammetry
University of Stuttgart
Geschwister-Scholl-Straße 24, D-70174 Stuttgart, Germany
Ph.: +49-711-121-4101, Fax: +49-711-121-3297
e-mail: dieter.kraus@ifp.uni-stuttgart.de

Commission V, Working Group 1

KEY WORDS: hybrid measurement system, 3d object reconstruction, feature extraction

ABSTRACT

The development of a digital photo theodolite system is a joint effort of the Geodetic Institute, University of Darmstadt, and the Institute for Photogrammetry, University of Stuttgart.

The system consists of a high resolution CCD line array camera mounted on a motor driven theodolite. The movement of the camera is synchronous to the theodolite movement with the two viewing directions parallel. A personal computer controls both the movement of the theodolite and the image acquisition process.

The intended area of application is close range scanning of facades and reliefs representing architectural objects or historical sites. The theodolite scans one line at a time and then repositions in a completely automated process. The scanning design allows imaging for a very wide scanning angle and makes it possible to scan interior rooms almost completely. Currently, the camera uses a CCD line sensor with 5000 pixels which leads to about 2 millimeters pixel size on the object at object distances of 10 meters. The positioning data of the theodolite can be used to determine the exterior orientation of each scan line very precisely.

The paper briefly introduces the system with its goals and then describes the research results obtained so far, which include

- the calibration of the relative orientation between camera and theodolite
- image corrections applied to the scan line image which include a pre-rectification process used to obtain images that follow approximately the standard camera model and a radiometric correction which minimizes the effects of different lighting conditions during the scan
- object reconstruction, 3D model generation and ortho image computation using the high resolution images
- automatic extraction of prominent object structures by image-based and height-model based approaches

1 INTRODUCTION

Nowadays, surveying of buildings for planning, monitoring or preservation purposes is done mainly by means of rulers, measuring tapes and theodolites. All those methods aim at the accurate determination of 3D point coordinates for a small number of representative object points which are later used to reconstruct the object in terms of simple primitives like polygons, planes, cuboids, cylinders etc. While these approaches have the advantage of a large data reduction since only a few points are required for the object description, they cause a number of problems as well. If the measured points are not selected and documented very carefully, the subsequent reconstruction may be impossible or erroneous. Also, if the object contains complex surfaces, an adequate description may not be possible using single points and geometric primitives. On the other hand, there is a growing demand for complete and accurate building reconstruction for planning and visualization purposes, which cannot be met by current measurement techniques.

Together with the Geodetic Institute of the University of Darmstadt, a hybrid measurement system is being developed. The system consists of a motorized tacheometer and a CCD line camera viewing in the same direction. While the tacheometer can be used for determining the exterior

orientation and the geodetic measurement of a few points, the system is also able to scan the building to obtain a high-resolution gray value image. Since the CCD line currently employed has 5000 sensor elements, the pixel resolution on the building is usually in the order of a few millimeters. To obtain a dense height map of the object, photogrammetric techniques for DTM production can be used. In this case, two or more images have to be taken. Work is under way to integrate a laser projector into the system as well, which would allow to obtain depth information using only a single standpoint.

So far, both research institutions have worked on system setup, scan procedures, calibration, image rectification, surface reconstruction, ortho image generation, and image segmentation. Due to the high resolution, the system is able to capture small object details.

2 DESCRIPTION OF THE HYBRID MEASUREMENT SYSTEM

For the Hybrid Measurement System (HMS) an electronic servo-driven tacheometer is used as turning and tilting platform. A CCD-line camera is mounted on the telescope of the tacheometer. For each scanned image line (with

5000 square pixels each, pixel size 7 micron) the measured tacheometer angles are transferred via interface together with the image data to a Personal Computer. The received data are currently processed on a Workstation, but it is planned to implement the algorithms onto a Notebook-PC.

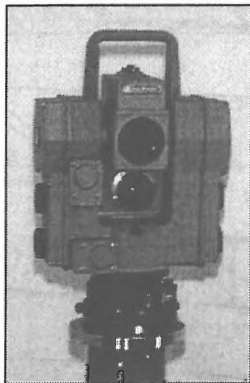


Figure 1: Hybrid Measurement System (HMS)

3 RESEARCH RESULTS

3.1 Calibration of the Relative Orientation Between Camera and Theodolite

For the calibration of the Hybrid Measurement System, a testfield was established within the Geodetic Institute, Darmstadt. It consists of about 150 target points distributed on a surface of ca. 40 m².

This testfield was scanned several times. The perspective center coordinates were determined by a resection algorithm using measurements with the tacheometer to the target points.

The determination of the calibration parameters was provided by a bundle adjustment (Hovenbitzer et al., 1998). These parameters are describing the relative translation between the optical center of the camera and the tacheometer center (X_0, Y_0, Z_0), the relative orientation between the visual axis of the camera and the visual axis of the tacheometer (φ, ω, κ) and the camera parameters itself (focal length c_K , principal point x_H , distortion parameters K_3, K_5 and K_7).

determined parameters	parameters	standard deviations value
X_0	-0.1 mm	0.1 mm
Y_0	28.2 mm	0.4 mm
Z_0	70.1 mm	0.1 mm
φ	-0.1479 gon	0.0044 gon
ω	-0.6833 gon	0.0011 gon
κ	0.0033 gon	0.0010 gon
c_K	35.758 mm	0.004 mm
x_H	0.482 mm	0.002 mm
K_3	-3.247810^{-5}	2.100410^{-6}
K_5	-2.536610^{-8}	1.444510^{-8}
K_7	-4.532910^{-11}	2.894810^{-11}

Table 1: first calibration results

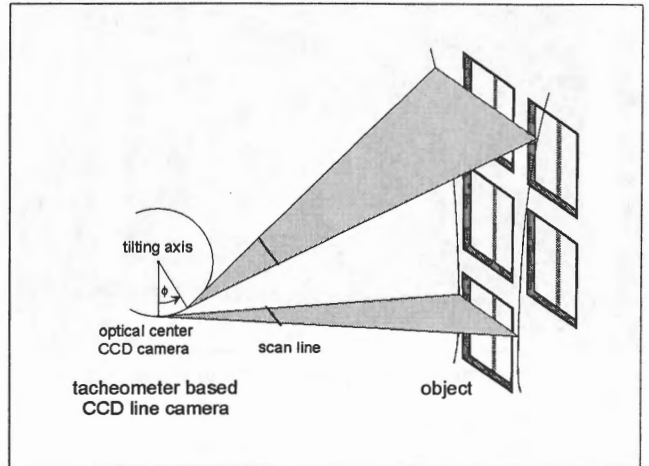


Figure 2: principle of HMS geometry

3.2 Image Corrections

By the construction of the HMS as a tacheometer with a CCD line camera positioned under the telescope, an image recording results by moving the projection center on a circular orbit (see Fig. 2).

The assembly of all image lines to a matrix leads to an image which is perspective only along the scan line direction (i.e. horizontal). Because of the rotation a cylindrical reference system is generated, whereby non-horizontal straight lines at the object are imaged as curves (see Fig. 3 and 4).

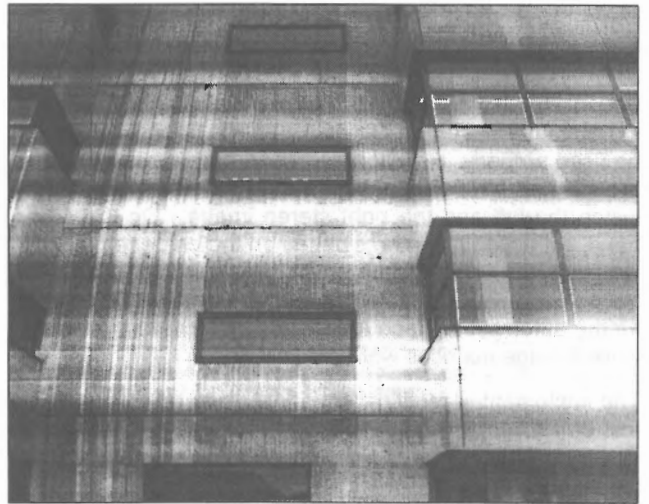


Figure 3: facade scan: original matrix of HMS

Thus, in the images the convergence of vertical (i.e. non-horizontal) parallel structures in the object space towards the upper image border is clearly noticeable which can be mathematical described by the equation:

$$x(\Phi) = \frac{C_1 \cdot \cos \Phi}{C_2 - \sin \Phi} \quad (1)$$

$x(\Phi)$ is the horizontal distance in the image, Φ the vertical angle, C_1 and C_2 are constants with $C_2 \gg 1$, which depend on the object distance, focal length and width of the object structure.



Figure 4: sandstone relief scan: original image matrix of HMS

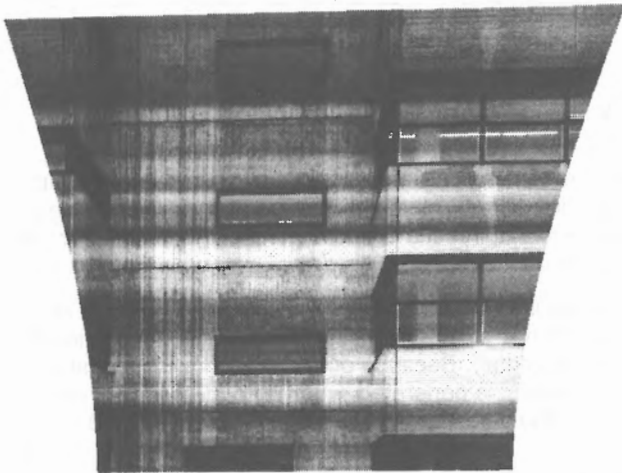


Figure 5: pre-rectified image "Facade"

Because of this distortion known procedures of digital photogrammetry based on projective image geometry cannot be used properly. Hereof area based matching algorithms are affected, which are using a simply modified relation between the left and the right stereo image. On the other hand, extraction algorithms based on the characteristics of the projective imaging (e.g. invariance of collinearity) cannot be used. But these procedures are essential elements for the automatic surface reconstruction. Therefore the received image matrices were pre-rectified in a first step.

The implemented rectification algorithm uses the parameters of the interior and exterior orientation provided by the system calibration for the computation of a spatial image ray for each image element.

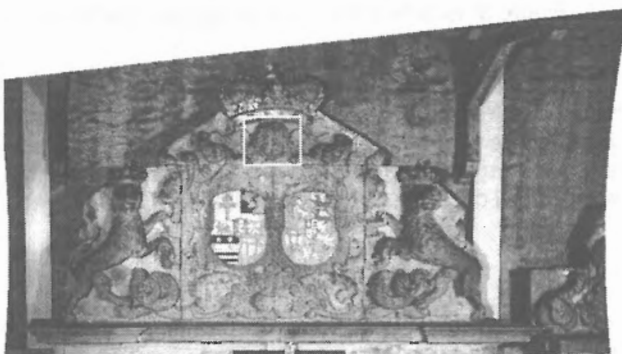


Figure 6: pre-rectified image "Relief"

The intersection points of all spatial image rays with an electible reference plain define a rectified image which approximates the image geometry of a pinhole camera model. Note: depending on the moving projection center and the unknown object surface, only an approximation of a rectified image is generated.

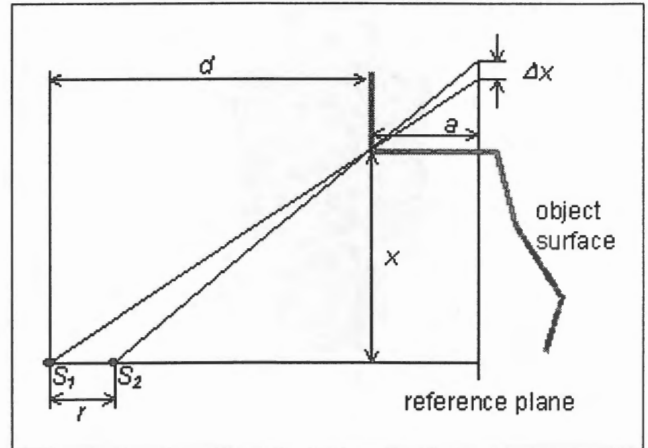


Figure 7: accuracy of image rectification

The estimation of the deviation to the strong perspective can be indicated as follows (Fig. 7):

$$\Delta x = \frac{a \cdot r \cdot x}{d \cdot (d - r)} \quad (2)$$

Δx is the error at the reference plane, a the maximum distance of the object relative to the reference plane (e.g. the facade), r the maximum distance between S_1 and S_2 (projection centers of the CCD line camera in the case of different vertical angles) and d the distance of the stand point of the HMS with regard to the object (all values in units of the object coordinate system).

For the image shown in Fig. 3 typical parameters are: $r \approx 51$ mm (4000 scan lines, upright angle 13 mgon per line, distance of the optical center from the tilting axis of the tacheometer 70 mm), $d \approx 12$ m, $x \approx 6$ m (aperture angle about 60 gon). If one now accepts $a = 1$ m, one receives a maximum error of $\Delta x = 2$ mm. If the rectified image is generated in a similar solution as the original image (5000 pixels per line), an error results of less than 0.9 pixels. Considering the fact, that S_1 and S_2 were accepted as projection centers located apart at a maximum distance, this error can be tolerated for image matching and line extraction – as investigations have shown. Fig. 5 shows the result of the pre-rectification for the facade scan (Fig. 3), Fig. 6 is the corresponding result for the test recording of a sandstone relief shown in Fig. 4. The elimination of the convergence of vertical parallel structures in the image is by far visible at the upper edge of the image.

3.3 Object Reconstruction, 3D Model Generation and Ortho Image Computation

3D object points are determined by an intersection algorithm. The therefore implemented algorithm uses the exterior and interior orientation of the HMS and the orientation data measured for each scan line by the tacheometer. For the generation of a grid digital surface model (DSM) homologous points were measured in a stereo image using area based image matching (see also 3.3.2).



Figure 8: ortho image "Head"

3.3.1 Ortho Image Generation For mapping purposes an ortho image generation algorithm was developed with respect to the special image geometry of the HMS. The algorithm works indirectly with anchor points and allows in this way the generation of ortho images at any resolution. Examples of generated ortho images are shown in Fig. 8 and Fig. 12.



Figure 9: result of stereo image matching for a part of the whole image

3.3.2 Object Reconstruction For the surface reconstruction of the scanned object homologous points of a stereo image pair received by the HMS were matched (see Fig. 9). Therefore an intensity based matching algorithm was used, which works with adaptive mask sizes (from 11x11 to 41x41 pixels) and image pyramids. The quality of the matched points were controlled by forward and backward matching. The amount of the good matchings (50 per cent) did not satisfy the expectations. The reasons for this results are:

- The in Fig. 3 shown facade was scanned out of doors under changing lighting. The resulting lighting differences between the single scan lines causes visible horizontal stripes in the images. Although the intensity based matching algorithm provides a radiometric correction of the matched masks, the dark/bright-patterns causes gradients, which lead to erroneous matching especially in the higher pyramid levels of the matching algorithm.

- The CCD line shows heavy differences of sensitivity for each pixel (PRNU). This results in vertical stripes in the images which reduce the efficiency of image matching and feature extraction.

A radiometric calibration of the sensor with regard to the lighting conditions during the scan procedure and/or a subsequent computational correction of the scan lines is expected to be a solution of these problems. No matter of these difficulties, very small object structures can still be registered with an accuracy of 1-2 mm in object space. Fig. 9 shows the result of image matching for a small section of relief (white frame in Fig. 6). White points indicate matched image points which were classified as "good" by the procedure. The bad point matching rate on the steep flanks left and right of the face indicates a misaligned relative orientation of the two images (for the present object).

3.3.3 3D Model Generation A procedure for generation of the standard format "VRML" with data of the HMS were developed. The generated files contain geometry and texture data. Fig. 10 shows some views of a generated model which can be viewed on a workstation in real-time.

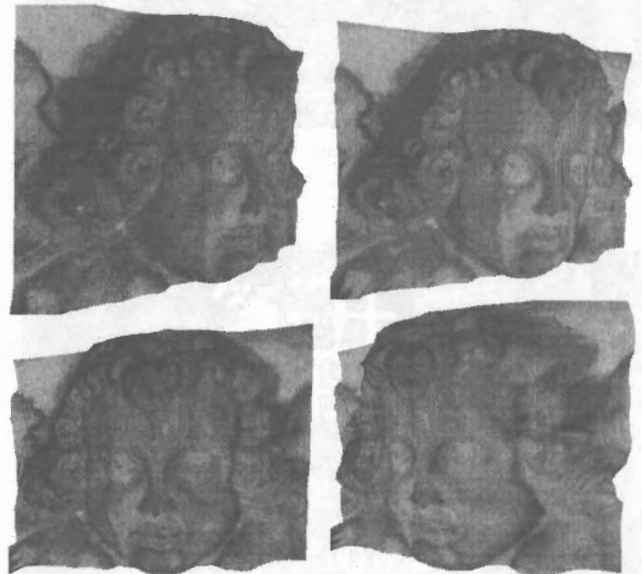


Figure 10: different views of VRML model "Head"

3.4 Automatic Extraction of Prominent Object Structures

The manual photogrammetric measurement of object structures for the generation of 3D-models of CAD (e.g. windows, joints) is very time-consuming. Accordingly, great savings on this field can be achieved during application of automatic procedures. Within the framework of our project, different procedures for segmentation were examined. Here, the enormous potential of the Hybrid Measuring System is visible because the HMS is able to image very fine structures at the object. The following procedures were used for image segmentation:

- Feature extraction using the Canny algorithm for discovering important object structures

- Segmentation using the Burns algorithm with subsequent grouping of line segments for extraction straight object structures.
- Segmentation by texture classification

3.4.1 Feature Extraction with Canny Procedure This standard procedure (Canny, 1986) extracts single points and can consequently not only be used on projective generated images. Therefore, the original high resolution images (5000 by 2800 pixels) were processed with this operator. With respect to the relationship between the original image and the ortho image the extracted points can be superimposed to the ortho image. Because of the high resolution of the Hybrid Measurement System very fine structures can be extracted (see Fig. 11 and Fig. 12).



Figure 11: scan image with superimposed extracted points (in black)



Figure 12: clipping of ortho image with superimposed extracted points (in black)

3.4.2 Segmentation by Burns Algorithm The known procedure after Burns (Burns et al., 1986) was used for the extraction of straight line segments. The procedure first segments the gradient image by grouping pixels of identical gradients into regions. These regions define a ramp in the intensity image which can be approximated by a plane for each area. The parameters of these planes are computed by a least squares algorithm from the intensity values within the segmented area. For the definition of the parameters of straight line segments, every plane defined in such a way is finally cut with a level plane of middle gray value. Since the

straight line segments are defined by this plane cut, and the plane parameters are determined by an homogenization from the gray values of an area, the procedure is able to determine the straight line with sub-pixel accuracy. Fig. 13 shows the line segments received by the algorithm processed with the pre-rectified facade picture from Fig. 5. In addition to the searched edges along the window frames also straight line segments are found within the windows and the facade itself. Unfortunately, it is especially difficult to segment the presented facade image, because both the horizontal stripes caused by illumination differences between the lines and the vertical stripes really existing at the facade itself generate line segments.

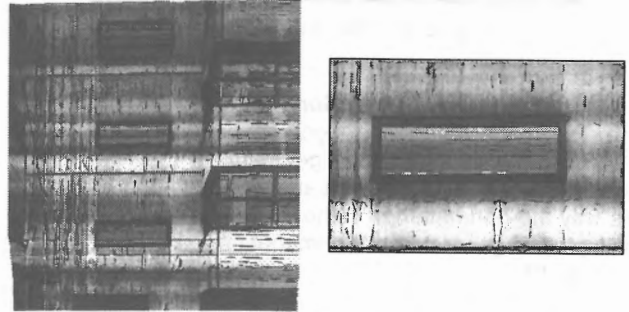


Figure 13: result of edge detection after Burns et al. (a) for the overall image (b) for the section close to the middle window

Partially, lines which are very close together are extracted by the algorithm. As a first step towards an extraction of window faces, the number of the lines was reduced when neighboring, collinear straight sections were summarized. Every straight section was included into a look-up window for ascertaining of possible combinations of lines. Within these look-up windows neighboring parallel line segments are searched. As candidates, those segments are chosen whose starting point is within the look-up window and which include a small angle with the straight line. If such segments are found, they are merged into a new line segment. The segment's position depends on the balancing straight line of all segments. Its start and end points are received by the projection of the summarized segments onto the harmonious straight line. Fig. 14 (a) shows the effect of this procedural step at the example of the pre-rectified facade image.

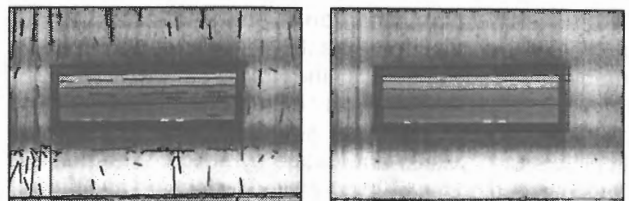


Figure 14: (a) Grouping line segments to longer straight sections. (b) Generated hypotheses for the situation of the window frame.

In a subsequent step, hypotheses for parallelograms were generated from the grouped line segments. The procedure defines for each line a field running parallel to that line having segments of the same direction. Since the dimensions of window faces can be defaulted coarsely at a facade, a strong reduction of possible combinations is attainable. The generated hypotheses are overlaid with the detail in Fig. 14 (b).

3.4.3 Segmentation by Texture Classification The segmentation of digital imagery using pixel-based algorithms causes problems, especially when different illuminations and viewing angles produce 'quasi' textural patterns. A more rigorous approach consists of the introduction of so-called texture channels. Texture is the spatial gray value variation in the environment of every image element. Texture channels represent computed vectors for every image element, describing the spatial gray value variation around this image element. Different texture measures such as statistical texture measures are derived from gray value dependence matrices. Co-occurrence matrices may describe the spatial relationship of gray values within an image matrix. It includes the standardized frequencies p_{ij} describing the spatial behavior according to distance and angle of pixel i and j . The representation of a such matrix can be used as a first interpretation of the original image. The more the engaged elements swath around the main diagonal itself, the more the image is uniform. However, the description of the texture is required for classification in the form of few representative values.

Therefore, texture features are computed from the gray value dependence matrices (Haralick et al., 1973). The following statistical texture parameters were computed and used:

Angular Second Moment

$$ASM = \sum_{i=1}^g \sum_{j=1}^g p_{ij}^2 \quad (3)$$

Contrast

$$CON = \sum_{i=1}^g \sum_{j=1}^g (i-j)^2 p_{ij} \quad (4)$$

Entropy

$$ENT = - \sum_{i=1}^g \sum_{j=1}^g p_{ij} \log p_{ij} \quad (5)$$

Inverse Difference Moment

$$IDM = \sum_{i=1}^g \sum_{j=1}^g \frac{p_{ij}}{1 + (i-j)^2} \quad (6)$$

In this case, g is the number of the gray values (i.e. the number of the rows and columns of the gray value dependence matrix) and p_{ij} are the standardized frequencies with $\sum_{i=1}^g \sum_{j=1}^g p_{ij} = 1$. The features were computed in horizontal and vertical direction delivering two different gray value dependence matrices. Fig. 15 - 18 show the result of calculation of these four features for a gray value dependence matrix (horizontal neighbor, distance one pixel) at the example of the rectified house facade.

The actual classification was carried out after the ISODATA method (Richards 1993). This non-checked classification determines the model classes automatically depending on a freely chosen rate of the image elements. The thematic meaning of the derived classes (wall, window etc.) is determined by the processor after the classification. The model classes are gained by the ISODATA method from the accumulations in the feature room (dot clouds and/or clusters). Every model class is featured by a mean value vector and the covariance matrix (signature of the class).

The procedure works iteratively. Starting from default class centers in the feature space (e.g. identical distributed) the

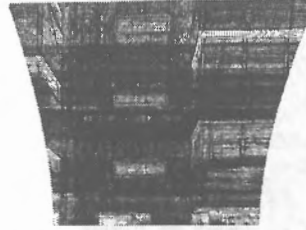


Figure 15: ASM (Eq. 3)

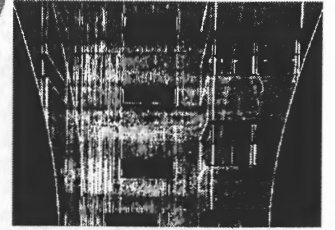


Figure 16: CON (Eq. 4)

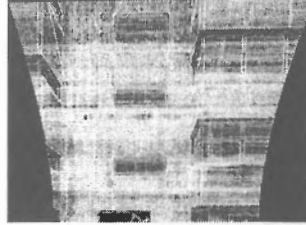


Figure 17: ENT (Eq. 5)

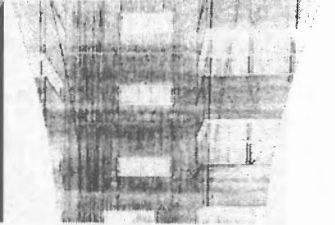


Figure 18: IDM (Eq. 6)

Figure 15 - 18: texture features by using of a co-occurrence matrix for horizontal neighborhood with distance 1

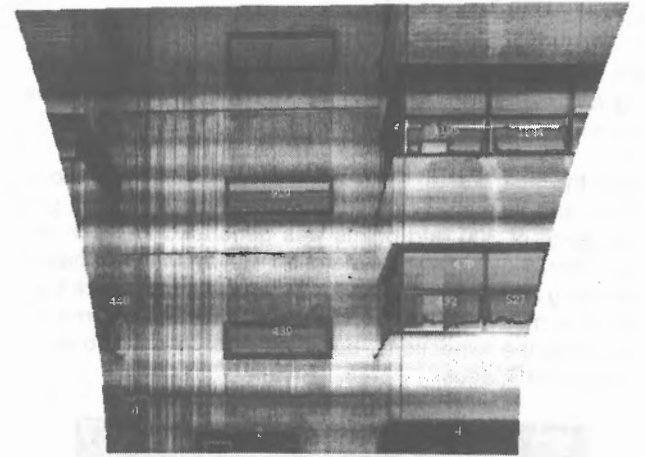


Figure 19: rectified image of facade and as window areas classified regions by the ISODATA algorithm

feature vectors of that class are assigned, which seems likely. In the next step, this center is determined again by means of the feature vectors assigned in the same way. As soon as the class centers do not change any further, the algorithm stops. Furthermore, criteria can be indicated, after which existing classes can be extinguished or new classes can be created. Fig. 19 shows areas which could be classified as window faces after carrying out the ISODATA algorithm. The image element-wise classification result was summarized into contiguous areas which were in turn subjected to selection criteria concerning form and size. Here, it must be mentioned again that the image material through the line-wise illumination differences is taken as difficult.

3.5 Image Quality

Because of the changing lighting conditions, it is necessary to improve the image quality. Therefore, new images were computed using a Fast Fourier Transform and a Gaussian high pass filter. So the long periodical changes between the image lines resulting from different light exposure were nearly eliminated (Fig. 20). For this example, the second

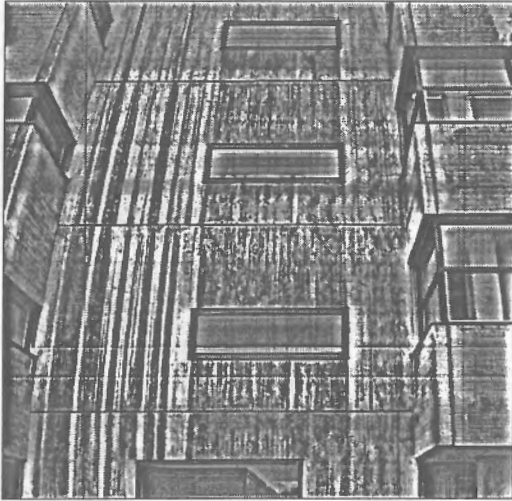


Figure 20: Improved image: less light exposure differences

pyramid level of a facade image was used. One can see that fast changings in light exposure cannot be corrected with this procedure properly.

It is expected that using these improved images the matching and extraction algorithms described above will work more reliable.

From the facade scan images, improved images were computed and in a subsequent step rectified. A regular grid consisting of 300 grid points was generated for each image. The grid points were matched with an intensity based matching algorithm (see 3.3.2). 218 of 300 points were successfully matched (Fig. 21: black dots) which is still not yet satisfying the expectations, but it is better than without improving the images.

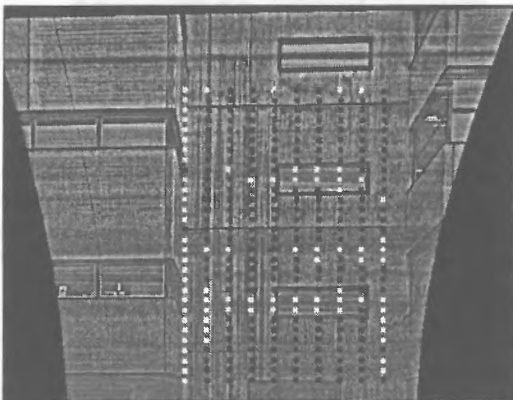


Figure 21: Improved and pre-rectified image: successfully matched grid points in black, other in white

4 ACKNOWLEDGEMENTS

This work is a part of a joint project of the Geodetic Institute, University of Darmstadt, and the Institute of Photogrammetry, University of Stuttgart. We gratefully acknowledge the support of the Deutsche Forschungsgemeinschaft (DFG), Bonn.

5 REFERENCES

- Burns, J., Hansen, A., Riseman, E., 1986. Extracting straight lines, *IEEE Trans. On Pattern Analysis and Machine Intelligence* 8(4), S. 425-443.
- Canny, J., 1986. A computational approach to edge detection. *IEEE Trans. On Pattern Analysis and Machine Intelligence* 8, S. 679-698.
- Fritsch, D., Kraus, D., 1997. Calibration of a CCD line array of a digital photo theodolite system. In: *Optical 3-D Measurement Techniques IV*, Wichmann-Verlag, Heidelberg.
- Haralick, R. M., Shanmugam, K., Dinstein, I., 1973. Textural features for image classification, *IEEE Trans. on Systems, Man, and Cybernetics*, Vol. SMC-3, No. 6.
- Hovenbitzer, M., Schlemmer, H., 1997. A line-scanning theodolite-based system for 3D applications in close range. In: *Optical 3-D Measurement Techniques IV*, Wichmann-Verlag, Heidelberg.
- Hovenbitzer, M., Schlemmer, H., Schmitt, J., Brenner, C., Fritsch, D., Kraus, D., 1998. Ein hybrides Messsystem zur visuellen, dreidimensionalen Koordinaten- und Formbestimmung in der Ingenieurvermessung. In: *Allgemeine Vermessungsnachrichten (AVN)*, 4/98, pp. 120-133.
- Richards, J. A., 1993. *Remote Sensing Digital Image Analysis*, Springer Verlag, Berlin Heidelberg.